# Study on the Preparation and Properties of MT-GE(6S-5-Methyltetrahydrofolate Calcium Salt Crystal Form C-Gelatin) Nanofiber Membrane

Yuhang Wang , Mochi Zhu , Yu Liu , Ke Wang , Tianyue Xu , Rui Duan , Junjie Zhang *

Posted Date: 6 April 2026

doi: 10.20944/preprints202604.0314.v1

Keywords: 6S-5-methyltetrahydrofolate calcium salt crystal form C; gelatin; nanofiber membrane

 doi:10.20944/preprints202604.0314.v1



*Article*

# Study on the Preparation and Properties of MT-GE(6S-5-Methyltetrahydrofolate Calcium Salt Crystal Form C-Gelatin) Nanofiber Membrane

**Yuhang Wang [b,d], Mochi Zhu [a,b], Yu Liu [a,e], Ke Wang [b,d], Tianyue Xu [a,b], Rui Duan [a,c,d] and Junjie Zhang [b,c,d]***

[a] School of Marine Science and Fisheries, Jiangsu Ocean University, Lianyungang 222005, China
[b] School of Ocean Food and Bioengineering, Jiangsu Ocean University, Lianyungang 222005, China
[c] Co-Innovation Center of Jiangsu Marine Bio-Industry Technology, Jiangsu Ocean University, Lianyungang 222005, China
[d] Jiangsu Institute of Marine Resources Development, Jiangsu Ocean University, Lianyungang 222005, China
* Correspondence: zjj203204@163.com

**Abstract**

Folate is an essential vitamin associated with protein and DNA synthesis in the body. Compared with synthetic folic acid, 6S-5-methyltetrahydrofolate calcium salt crystal form C (MTHF CAC) is safer and has a higher bioavailability. In this study, a nanofiber membrane (MT-GE) was prepared from fish gelatin and MTHF CAC in the aqueous system via electrospinning. The differential scanning calorimetry results show the higher thermal stability of MT-GE than GE. The weight loss curve of MT-GE detected by thermogravimetric analysis was higher than that of GE. X-ray diffraction indicated the slightly higher crystalline strength of MT-GE than GE. Therefore, the inclusion of MTHF CAC improved the physical characteristics of GE nanofibers. High-performance liquid chromatography analysis revealed that the retention of MTHF CAC in MT-GE reached 85.57%, which suggests that electrospinning caused no effect on the properties of MTHF CAC. The MT-GE membrane supported cell proliferation, and the Cell Counting Kit-8 results indicate that the cell proliferation rate exceeded 100%, with the MT-GE solution demonstrating more than double the proliferation rate of the control group. Therefore, MT-GE has great potential for use as medical biomaterial.

**Keywords:** 6S-5-methyltetrahydrofolate calcium salt crystal form C; gelatin; nanofiber membrane

## 1. Introduction

Electrospinning is a technique where polymer solutions or molten polymers are stretched into nanofibers by a high-voltage electrostatic field (Anu Bhushani & Anandharamakrishnan, 2014; Wen et al., 2016). Nanofiber membranes have huge specific surface area and porosity (Lee et al., 2008; Stitzel et al., 2006; Weiwei et al., 2008), as well as a high degree of designability in composition and structure (Wang et al., 2021), making electrostatic spun fiber membranes promising for applications in biomaterials, tissue engineering, drug sustained release, etc (Herrero-Herrero et al., 2018).

Gelatin is approved by the Food and Drug Administration as one of the most commonly used biopolymers due to its excellent biocompatibility, degradability, and wide applicability (Karim & Bhat, 2008). At present, the gelatin used in electrospinning mainly originates from the skins of porcine and cattle. Nanofiber membranes, which are produced by electrostatic spinning of a gelatin solution derived from porcine skin and 2,2,2-trifluoroethanol as the solvent, exhibit exceptional thermal stability and mechanical properties, which make them a promising scaffold material for tissue engineering (Zhang et al., 2006). The nanofiber mats made using cattle skin gelatin showed a positive effect on the cell proliferation of human dermal fibroblast and embryonic kidney cells (Erencia et al., 2015). Compared with gelatin of mammalian origin, fish gelatin has a lower zoonotic risk and fewer

 doi:10.20944/preprints202604.0314.v1



religious restrictions (An et al., 2010; Arfat et al., 2016; Padrão et al., 2014; Padrão et al., 2015). Kwak (Kwak et al., 2017) produced ultrafine nanofiber webs using an aqueous solution of cold-water fish gelatin through electrostatic spinning. The nanofibers demonstrated higher cell adhesion and proliferation rates compared with those made from mammalian gelatin. Songchotikunpan (Songchotikunpan et al., 2007) developed an acidic system of ultrafine fish-gelatin nanofibers that were subsequently treated with glutaraldehyde. The resulting nanofibrous membranes exhibited improved water resistance and showed a high potential for use in the biomedical industry.

Folate is an essential vitamin associated with protein and DNA synthesis in the body and serves as a methyl donor in one-carbon metabolism (Bentsen et al., 1981; J, 2002). Currently, in addition to synthetic folic acid, crystalline forms of folate include 6S-5-methyltetrahydrofolate calcium salt crystal form C (MTHF CAC), (6S)-5-methyltetrahydrofolic acid, and glucosamine salt. Compared with synthetic folic acid, MTHF CAC is safer and more available to the body (J et al., 2003; Klaus et al., 2010). Zhou (Zhou, 2014) reported that folic acid protected against delayed healing of skin wounds in mice with diabetes and contributed to tissue regeneration (Ahu et al., 2019). Bagheri pointed out that the main reason for slow wound healing in diabetic patients is the lack of NO in the body. NO is a critical signaling molecule essential for normal wound repair. Folate had the homocysteine-lowering effects and antioxidant actions, which had a healing effect on diabetic wounds (Mansooreh et al., 2011). Hybrid electrospinning of porcine skin gelatin and synthetic folic acid was used to produce a fibrous membrane with excellent biocompatibility for tissue engineering and wound healing (Nur et al., 2021). However, the reports on electrospun membrane prepared from MTHF CAC and gelatin, especially fish gelatin, were limited.

Some organic solvents such as TFA, HFIP, etc. were usually employed in the most spinning process (Arumugam et al., 2024; Nur et al., 2021; Pathum et al., 2021). Since MTHF CAC was insoluble in the organic solvents, in the present study, the nanofiber membrane (MT-GE) with the components of fish gelatin and MTHF CAC was prepared in the aqueous system through electrospinning. Its morphological characteristics, thermal properties, and crystal structure were investigated, and its cytotoxicity was evaluated. This research provides basic information on the characteristics of MT-GE which could be a new kind of biomaterial as the medical dressings .

## 2. Materials and Methods

### *2.1. Materials*

Fish gelatin was provided by the Collagen Laboratory of Jiangsu Ocean University. 6S-5-methyltetrahydrofolate calcium salt crystal form C (MTHF CAC) was provided by Lianyungang Jinkang Hexin Pharmaceutical Co., Ltd, China. NIH-3T3 cells, purchased from the Kunming Cell Bank of the Typical Culture Collection Committee of the Chinese Academy of Sciences, China. Trypsin-EDTA (0.25%) containing phenol Red, purchased from GIBICO, China. CCK-8 kit, penicillin/streptomycin solution, DMEM medium, fetal bovine serum, phosphate buffer solution, and other reagents were purchased from Sangon Biotech Co., Ltd, China.

### *2.2. Methods*

#### 2.2.1. Preparation of Electrospinning Solution and Electrospinning

Nanofibers were prepared using an electrostatic spinning device (DP30, Yunfan Technology Co., Ltd., Tianjin, China). Gelatin solution was prepared according to the method of Songchotikunpan etc (Songchotikunpan et al., 2007). The gelatin was dissolved in 40% (v/v) acetic acid aqueous solution to obtain the gelatin solutions at a concentration of 15% (w/v). 4mg MTHF CAC was mixed into the gelatin solutions with the final concentration of 0.4%(w/w). The solution was loaded into a 5 mL plastic syringe with a stainless steel needle and pumped at a flow rate of 0.315 mL/h. The metal needle size of the syringe was 18 G with a nominal inner diameter of 0.84 mm and an outer diameter of 1.27 mm. A positive voltage of 20 KV was used, and the tip-to-collector distance was 15 cm. The collection

 doi:10.20944/preprints202604.0314.v1



time was fixed at 127 min. All measurements were carried out in triplicate at room temperature (25±1℃). Gelatin nanofibers (GE) were prepared by the same method as a control.


**Figure 1.** The electrostatic spinning process of MT-GE**.**

2.2.2. Rheological Properties of Electrospun Solutions

The rheological properties of the spinning solution were determined using a rheometer (MCR102, Anton Paar, Germany) at 25±1℃ with a rotor diameter of 25 mm. Each sample was equilibrated for 5 min before testing. To avoid evaporation of the sample, light silicone oil was applied to the gap between the rotor and the measuring disc (Wongsasulak et al., 2014). The shear rate was set in the range of 1-1000 s-1 (Huang et al., 2018).

2.2.3. Scanning Electron Microscopy (SEM)

Both samples of gelatin electrospun film (GE) and MT-GE were surface sprayed with gold by ion sputtering instrument (SBC12, Beijing CSCI Technology Co., Ltd., China). The samples were morphologically characterized by cold field emission scanning electron microscopy (Regulus8100, Hitachi Limited). Origin2018 software was used to statistically analyze the diameter distribution of nanofibers.

2.2.4. Fourier Transform Infrared Spectroscopy (FTIR)

The electrospun films were scanned and analyzed by Fourier infrared transform spectroscopy (FT-IR Spectrometer, Perkin Elmer, America). The scanning range was 4000 to 400 cm-1 with an interval of 1 cm-1 and a resolution of 4 cm-1 (Choi et al., 2015; Ghorani et al., 2020).

2.2.5. Differential Scanning Calorimetry and Thermogravimetry Analysis (DSC and TGA)

The thermal properties of the nanofiber membranes were analyzed with a simultaneous thermal analyzer (STA8000, Perkin Elmer, America) to determine the DSC and TGA parameters of different samples. The samples were weighed in a crucible and warmed up from 30℃ to 400℃ at a ramp rate of 10℃/min in a gaseous environment with a nitrogen flow rate of 20 mL/min (Qin et al., 2019).

2.2.6. X-Ray Diffraction Analysis (XRD)

An X-ray diffractometer (X'Pert Powder, PANalytical B.V., Netherlands) was used to analyze the crystallinity variation of MT-GE. The XRD system was operated at a scan range of 2θ =5 °-40 °, 20 KV, and 5 mA, K$\alpha$ ($\lambda$=1.5418 ), a rate of 4 °/min, a step of 0.02 ° (Ki et al., 2005; Qin et al., 2019).

2.2.7. Determination of the Loading Rate of MTHF CAC

The MT-GE was dissolved in 1 mL of ultrapure water. Vc was added at the ratio of 1:1 (w/w) of MTHF-CAC and dissolved thoroughly. The solution was added to the extractant (1-Butanol:Trichloromethane=1:4) at the ratio of 9:1. The protein was removed by centrifugation at 6000

 doi:10.20944/preprints202604.0314.v1



rpm/min for 10 min, and the supernatant was then filtered at 0.22 μm membrane (DUAN et al.). MTHF CAC retention rate was determined by HPLC. The chromatographic column of HPLC was a C18 column, 250 mm×4.6 mm, with a particle size of 5 μm. The mobile phase was 35% methanol solution at a flow rate of 1.1 mL/min. The detection wavelength was 280 nm. The injection volume was 10 μL. The column temperature was 32℃. And the acquisition time was 33 min.

2.2.8. Cytocompatibility Evaluation

Samples were tested for cytotoxicity. NIH3T3 cells were cultured in complete medium (89% (v/v) DMEM, 10% (v/v) fetal bovine serum (FBS), and 1% (v/v) penicillin/streptomycin) at 37℃ in 5% CO2. NIH-3T3 cells growing at 80-90% confluence at the bottom of T25 culture flasks were digested with trypsin. A cell suspension of approximately 5×104 cells/mL was prepared. A 96-well plate was taken and 100 μL of cell suspension was added to the sample and control groups, 3 replicate wells for each group. After 24 hours of incubation, 100 μL of the sample to be tested (sample group) or 100 μL of complete medium (control group) was added to each well. Samples were prepared in complete medium with MT-GE solutions at concentrations of 2, 4, 8, 10, and 14 mg/mL, respectively. After 24 hours of incubation, 10 μL CCK-8 was added. After 1 hour of incubation, the OD value was measured at 450 nm (complete medium was used as the blank group), and the cell proliferation rate was calculated according to the following formula:

$$Cell\ proliferation\ rate(\%) = \frac{(A - A_0)}{(A_1 - A_0)} \times 100\%$$

The formula:
A - OD450 value of the sample group;
A0 - OD450 value of the blank group;
A1 - OD450 value of the control group.

2.2.9. Statistical Analysis

All data graphs were designed by Origin 2018 (Microcal, USA) and the data were statistically analyzed by IBM SPSS Statistics 20 (IBM, USA).

## 3. Results and Discussion

### *3.1. Morphological Characteristics*

Figure 2 showed the scanning electron microscopy (SEM) and diameter distribution results of MT-GE and GE. The GE nanofibers had a beadless and smooth surface(Figure 2A) while MT-GE had a rough mesh structure was formed (Figure 2C). The SEM results showed that the diameters of GE fiber and MT-GE were mainly distributed in the ranges of 411.87±29.21 nm and 314.99±10.54 nm, respectively (Figs. 2E and 2F). The difference in the morphology and diameters of the two samples was mainly attributed to the dissimilarity of rheological properties of the electrospun solution (Figure 2G). The gelatin solution was a non-Newtonian fluid and its viscosity was determined by the shear rate. The viscosity of the solution decreased with increasing shear rate, which exhibited shear-thinning behavior (Ding et al., 2002; Doshi & Reneker, 1995; Sun et al., 2023). The MT-GE blends were 5.67%–12.09% less viscous than GE for shear rates in the range of 200–1000s-1.

 doi:10.20944/preprints202604.0314.v1



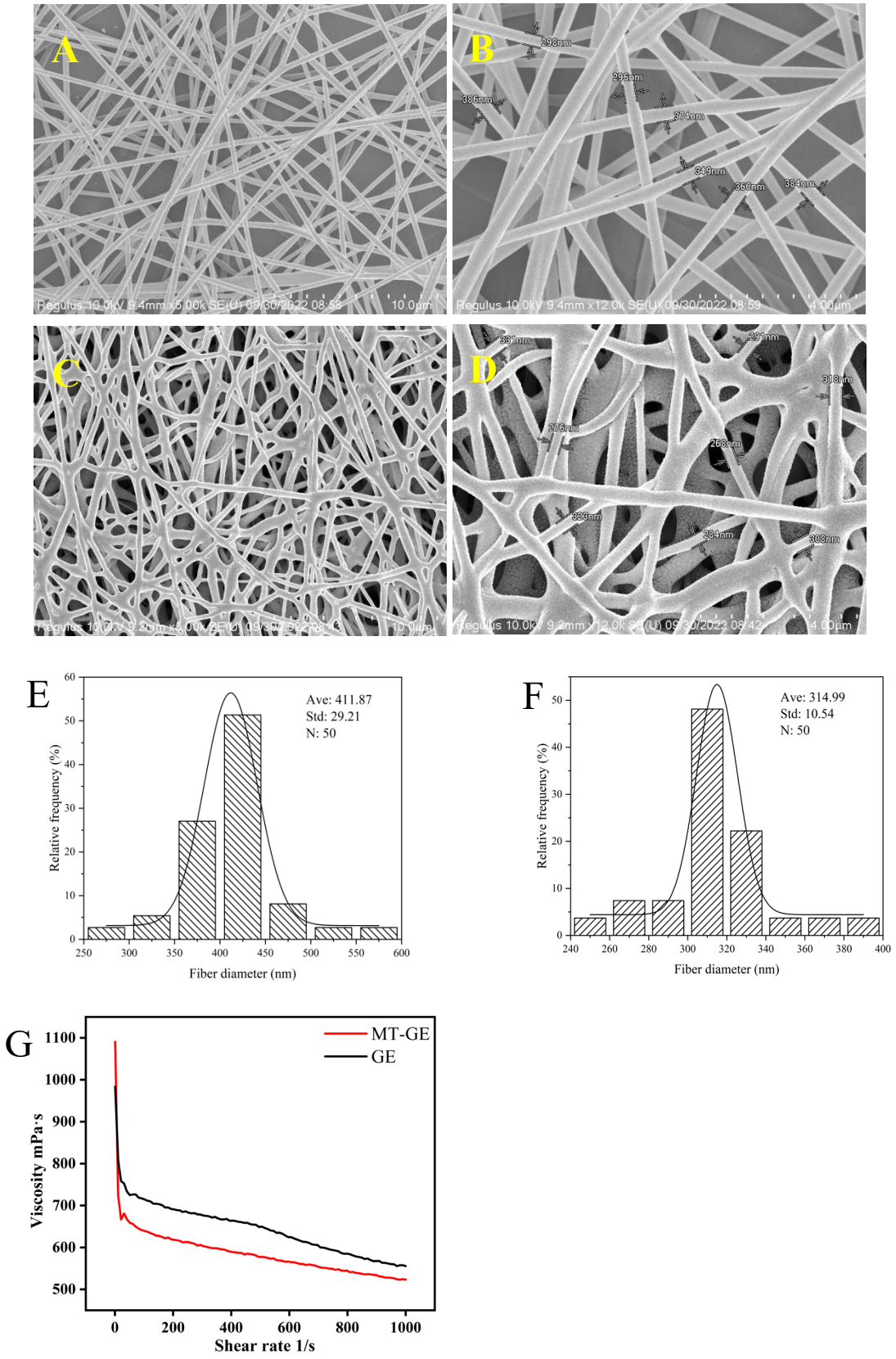


**Figure 2.** SEM results and diameter distribution statistics of MT-GE and GE. (A)GE Nanofibers (Magnification: 5 KX, scale bar: 10μm). (B) GE Nanofibers (Magnification: 12 KX, scale bar: 4μm). (C) MT-GE Nanofibers (Magnification: 5 KX, scale bar: 10μm). (D) MT-GE nanofibers (Magnification: 12 KX, scale bar: 4μm). (E) Statistical results of GE diameter distribution. (F) Statistical results of MT-GE diameter distribution. (G) Shear rate-viscosity curve.

 doi:10.20944/preprints202604.0314.v1



In the e-spinning process, as the viscosity of the spinning solution decreased, the evaporation rate would increase. The fibers could be cured and shaped faster in air, resulting in the formation of finer fibers (Sun et al., 2023). However, if the solvent evaporated too fast, insufficient stretching would occur and the curved and irregular fibers formed (Lei-Gen & Ji-Huan, 2017). The decrease of MT-GE viscosity might be due to the fact that the calcium ions in MTHF CAC solution could bridge the negatively charged carboxyl groups in the gelatin (Figure 3), which reduced the electronic repulsion (Jiahui et al., 2022; Xiaoran et al., 2008). Therefore, compared with the spinning solution of GE, that of MT-GE evaporated faster, thus the electrospun fibers had smaller diameter and lower uniformity.

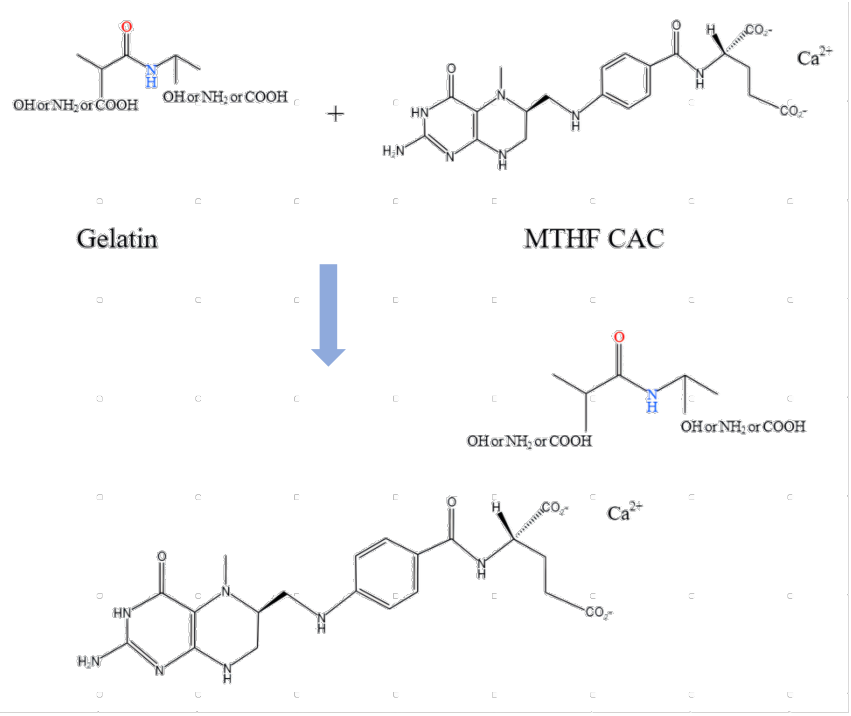


**Figure 3.** Mechanism reaction of Gelatin with MTHF CAC.

*3.2. Fourier Transform Infrared Spectroscopy (FTIR)*

Figure 4 showed the FTIR spectrum of MT-GE and GE. MT-GE and GE had major characteristic peaks in the amide A band at 3285 cm-1, in the amide Ⅰ band at 1647 cm-1, in the amide Ⅱ band at 1539 cm-1, and in the amide Ⅲ band at 1241 cm-1 and in the amide Ⅳ band at 653 cm-1. The amide A and I-Ⅲ bands were the major characteristic peaks that prove the peptide chain backbone structures of a protein (Lingling et al., 2021). The formation of hydrogen bonds caused the wave number of the amide A band (3400-3440 cm-1) to blueshift to about 3300 cm-1 (Chen et al., 2016; Chen et al., 2008). The slight decreased in transmittance of the band at 3285 cm-1 corresponding to -OH functional group, might indicate of the formation of hydrogen bonds between gelatin and MTHF CAC (Bustos et al., 2022; Katouzian et al., 2020). The strength of the amide bonds of MT-GE was weaker than that of GE (reduced peak heights in the amide A, amide I, amide II, amide Ⅲ and amide Ⅳ bands), might be because the -COOH groups in the gelatin molecule form ionic bonds with calcium ions in the MTHF CAC(Figure 3), providing nucleation sites for inorganic crystal growth.

 doi:10.20944/preprints202604.0314.v1



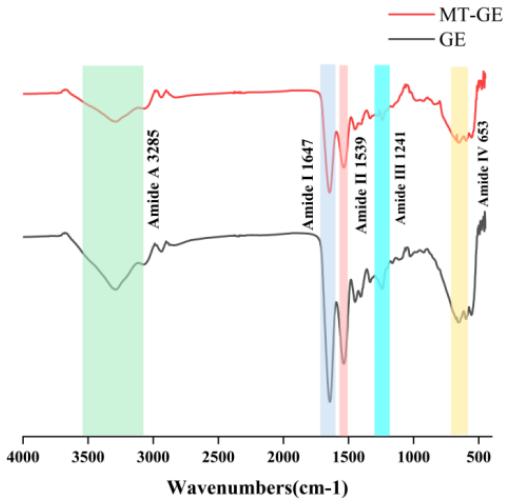


**Figure 4.** FTIR scan spectra of MT-GE and GE.

The FTIR spectra of PLLA/catfish skin gelatin nanofibers showed that with the increase of PLLA proportion in the electrospinning solution, the molecular interactions between gelatin and PLLA became weaker (An et al., 2010). This might be attributed to that PLLA lacked -OH groups binding to -NH2 groups in gelatin to form hydrogen bonds. In contrast, fish gelatin contained a large amount of -OH, -NH2, and -COOH, and MTHF CAC molecules contained -COOH and -OH groups. Gelatin and MTHF CAC could form a lot of hydrogen bonds, which led to the further formation of a relatively stable structure of MT-GE.

*3.3. Differential Scanning Calorimetry and Thermogravimetry Analysis (DSC and TGA)*

Figure 5A indicated the DSC results for MT-GE and GE. Two obvious heat absorption peaks for MT-GE and GE appeared. The first heat absorption peak was the denaturation temperature of MT-GE and GE, which were 80.21°C and 66.99°C, respectively. The Td of SPC/gelatin nanofibers prepared by Vahid et al was 74.41℃ (Katouzian et al., 2020), which was lower than that of MT-GE (80.21℃). The second heat absorption peak was the melting points of MT-GE and GE, which were 292.88°C and 288.50°C, respectively. The thermal stability of MT-GE was higher than that of GE, probably due to the reaction between -OH in the MTHF CAC molecule and -COOH in the gelatin. The crosslinking between the molecules led to an increase in hydrogen bonds and van der Waals forces, which increased the enthalpy of the material (Chen et al., 2016; Chen et al., 2007; Fabián et al., 2022; Jiahui et al., 2022; Katouzian et al., 2020; Lingling et al., 2021; MOU et al., 2018; Vahid et al., 2022).

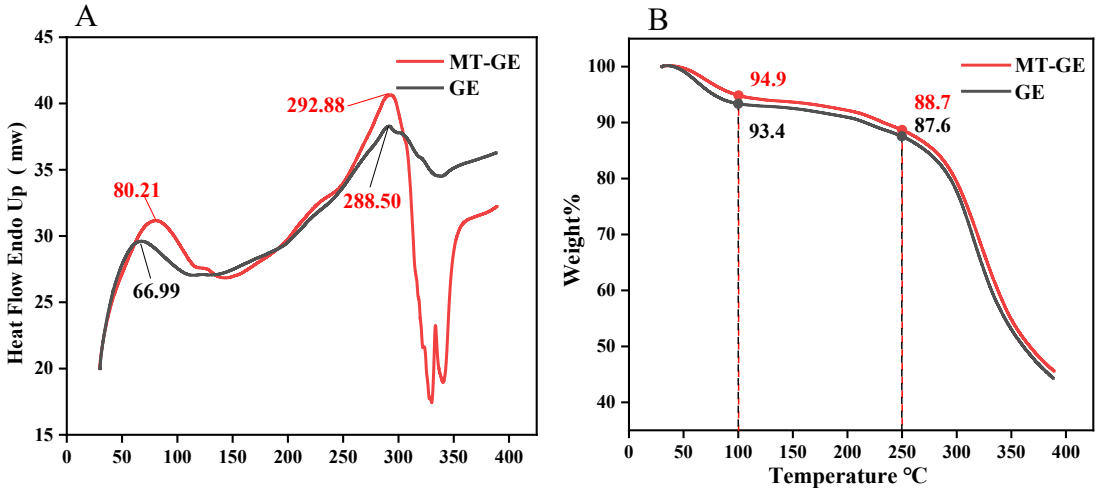


**Figure 5.** DSC and TGA weight loss curves of MT-GE and GE.

 doi:10.20944/preprints202604.0314.v1



Figure 5B showed the TGA results for MT-GE and GE. The thermal degradation process could be divided into two phases, the first phase being the depolymerization of the macromolecular network, and the second phase being the further degradation after breaking the intermolecular covalent bonds. Figure 5B showed a rapid decrease in the mass of the fiber film in the range of 50℃-100℃ due to the depolymerization of the macromolecular network with rapid water loss. The mass of MT-GE in the range of 200℃-250℃ decreased slowly. The spatial structure of the molecules changed, and heat-absorbing dissociation of the intramolecular crystalline water occurred (Torres-Giner et al., 2008). TGA results showed residual weights of MT-GE and GE were 95.9% and 93.4% at 100℃, respectively, while those of two samples were 88.7% and 87.6% at 250℃., respectively. The weight loss curve of MT-GE was slightly higher at all tested temperatures, indicating that the thermal properties of MT-GE were higher than that of GE. These results were accordant to those achieved by DSC.

*3.4. X-Ray Diffraction Analysis (XRD)*

Figure 6 showed the X-ray diffraction patterns of MT-GE and GE. One distinct peaks appeared at 2θ=7.12°,which represented the helix conformation in gelatin (Bigi et al., 2004). The gelatin nanofiber film showed a smaller peak at 2θ=11.6°. The inclusion of MTHF CAC significantly amplifies the vibration of this peak, which might be due to the introduction of salt in the preparation solutions (Anita et al., 2021). The peak arround 20.94° represented the amorphous region. With the conversion of collagen into gelatin, the original intact triple helix gradually disintegrated, and the amorphous structure gradually increased, resulting in a broad peak in the diffractogram (Badii et al., 2014). Figure 6 showed the addition of MTHF CAC did not introduce new peaks in the fiber membrane, the crystalline strength of MT-GE was slightly higher than that of GE, indicating that the addition of MTHF CAC favored the formation of crystalline structure. The result was in accordance with that of the DSC.

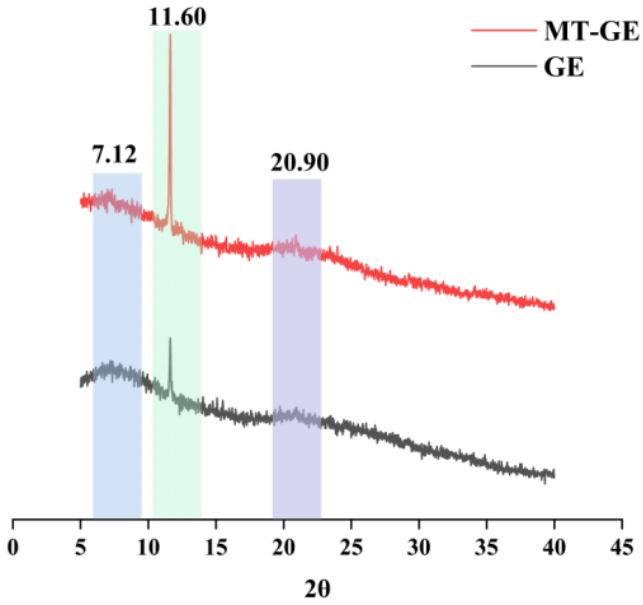


**Figure 6.** X-ray diffraction patterns of MT-GE and GE.

*3.5. Determination of the Loading Rate of MTHF CAC*

To investigate the stability of MTHF CAC in MT-GE, the loading rate of MTHF CAC was determined by HPLC. Figure 7 showed the HPLC profiles of MTHF CAC and MT-GE. MTHF CAC had strong UV absorption at 280 nm, and the standard curve could be obtained by measuring the peak area via HPLC as $\gamma = 21759\alpha + 7386.3$ (R2=0.9997, where γ is the peak area, and $\alpha$ is the concentration), with good linearity in the concentration range of 0.2–8 μg/mL. Its characteristic peak retention time was about 15.6 min (Figure 7A). MT-GE was measured by HPLC after pretreatment,

 doi:10.20944/preprints202604.0314.v1



and it also showed a characteristic peak at about 15.6 min (Figure 7B). The peak shape of MT-GE was good, and no other unknown peaks were observed near it. Therefore, the peak was determined as the characteristic peak of MTHF CAC. This finding demonstrated that MT-GE was successfully piggybacked on MTHF CAC. The calculated concentration of MTHF CAC was 6.37 μg/mL, indicating that the loading rate of MTHF CAC in MT-GE was 85.57%. MTHF CAC was not fully loaded in MT-GE, probably due to a small loss of MTHF CAC from the pre-treatment process before electrospinning. The choice of nanofiber matrix played a key role in the release effect (Leung et al., 2015). This result showed that fish gelatin had excellent carrier matrix piggybacking effect. The electrostatically spun MT-GE fiber membrane not only improved the thermal stability of MTHF CAC but also rapidly released the active ingredients of MTHF CAC from the carrier. It provided a good property basis for the application of MT-GE as a biomolecule material.

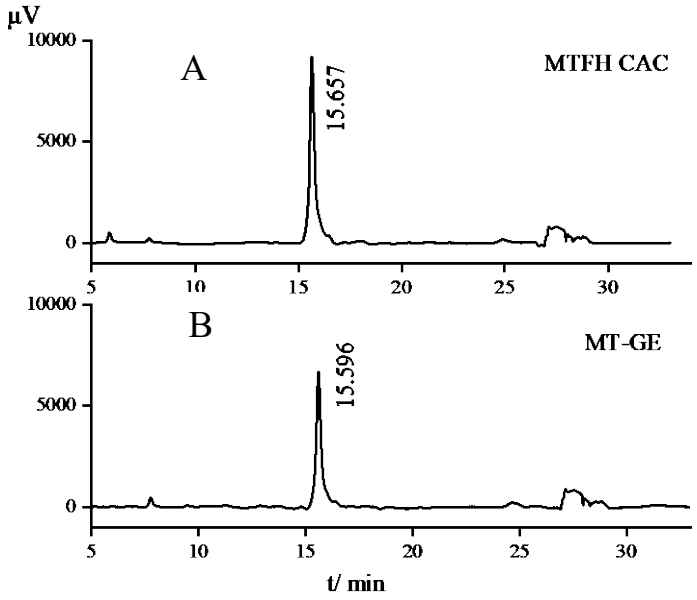


**Figure 7.** (A) 7.44 μg/mL of MTHF CAC solution. (B) MT-GE solution after deproteinization.

*3.6. Cytocompatibility Evaluation*

Fibroblasts were commonly used in the evaluation and development of tissue engineering materials due to their rapid differentiation and regeneration properties (Bashur et al., 2006; Ekaputra et al., 2011). The in-vitro cytotoxicity tests of MT-GE nanofibers toward NIH3T3 cells were evaluated using CCK-8 assays. Figure 8 showed that the cell viabilities for 24 h were over 100% at all test concentrations up to 14 mg/mL, revealing the non toxicities of MT-GE toward cells. The cell viabilities at the concentration of 8 mg/mL MT-GE and GE solution was 158.8% and 116.3 %, respectively. When the concentration reached 14 mg/ml, the cell proliferation rate of MT-GE was 1.87 times than that of GE. It is well known that gelatin is a gold standard material for tissue engineering due to its good biological recognition. Due to the presence of arginine-glycine-aspartic acid sequences (RGD), this protein is able to improve cell adhesion, mimicking the major biochemical signals that are present into the cell microenvironment (Ambrosio et al., 2012). Folate played a vital role in the growth and repair of cells, aiding wound healing by synthesising nucleic acids (Ahu et al., 2019; Duthie & Hawdon, 1998; Mansooreh et al., 2011). It could promote cell proliferation by upregulating the expression of proteins, such as Cyclin A2 and vascular endothelial growth factor (VEGF) (Li et al., 2013). Additionally, folic acid also could activate the Notch signaling pathway, which regulated cell proliferation, differentiation and apoptosis, leading to increased expression of receptors Notch1 and signaling molecules Hes5 and thereby promoting cell proliferation (Liu et al., 2010).

 doi:10.20944/preprints202604.0314.v1



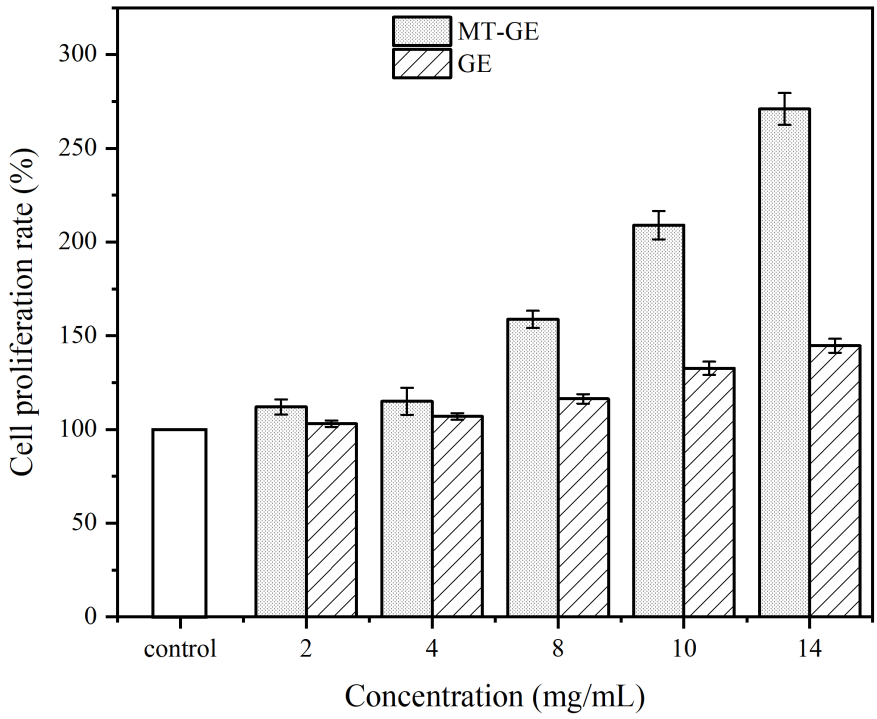


**Figure 8.** Effect of different concentrations of MT-GE and GE solution on cell proliferation.

Fatma,etc. prepared PVA/Gel nanofiber membrane and the proliferation rate of of L929 cells was 82.99%(Nur et al., 2021). The FCP scaffolds obtained by electrospinning 10% (w/v) collagen and 10% (w/v) PCL showed 95% proliferation rate of HaCaT cells (Pathum et al., 2021). The proliferation rate of the SF/CL scaffolds prepared by e-spinning of collagen and filipin proteins was only 65% for NIH3T3 cells (Arumugam et al., 2024). Therefore, the nanofiber membrane prepared from fish gelatin and MTHF CAC had better biocompatibility and could be an appropriate candidate of wound dressing.

## 4. Conclusions

In this study, MT-GE blends were prepared by electrospinning MTHF CAC and gelatin in the aqueous system to obtain the nanofiber membrane. The viscosity of MT-GE electrospun solution was lower than that of GE. The FTIR spectrum showed the formation of hydrogen bonds between gelatin and MTHF CAC. The X-ray diffraction pattern indicated a slight enhancement in the crystallinity of MT-GE. The results of DSC and TGA showed the thermal stability of MT-GE was higher than that of GE, which was in agreement with the results of XRD. MT-GE could enhance the supported cell proliferation,when the concentration of MT-GE solution reached 14 mg/mL, the cell proliferation rate was 2.71 times higher. Therefore, the MT-GE nanofiber membranes prepared from fish gelatin and MTHF CAC, had great properties to be a candidate of wound dressing.

**Acknowledgments:** This work was supported by Postgraduate Research & Practice Innovation Program of Jiangsu Province (KYCX2023-123), Innovation and Entrepreneurship Training Program for College Students in Jiangsu Province (SY202111641638005) and the A Project Funded by the Priority Academic Program Development of Jiangsu Higher Education Institutions (PAPD) . We are grateful to Lianyungang Fiber New Material Research Institute Co. for their help in this study.

## Reference

 doi:10.20944/preprints202604.0314.v1




1. P. Ahu, T. Feriha, K. Aslıhan, M.H. Koray, B. Yasemin, E. Hülya, A. Osman, Role of mesenchymal stem cell-derived soluble factors and folic acid in wound healing, *Turk. J. Med. Sci.* 49 (2019) 914–921.
2. L. Ambrosio, A. Gloria, V. Guarino, M.G. Raucci, Hydrogel-based platforms for the regeneration of osteochondral tissue and intervertebral disc, *Polymers* 4 (2012) 1590–1612.
3. K. An, H. Liu, S. Guo, D.N.T. Kumar, Q. Wang, Preparation of fish gelatin and fish gelatin/poly(l-lactide) nanofibers by electrospinning, *Int. J. Biol. Macromol.* 47 (2010) 380–388.
4. R. Anita, A. Hadi, Z. Zahra, G. Ahmad, M. Esmaeil, Collagen/chitosan-functionalized graphene oxide hydrogel provide a 3D matrix for neural stem/precursor cells survival, adhesion, infiltration and migration, *J. Bioact. Compat. Polym.* 36 (2021) 296–313.
5. J. Anu Bhushani, C. Anandharamakrishnan, Electrospinning and electrospraying techniques: potential food based applications, *Trends Food Sci. Technol.* 38 (2014) 21–33.
6. Y.A. Arfat, S. Benjakul, T. Prodpran, P. Sumpavapol, P. Songtipya, Physico-mechanical characterization and antimicrobial properties of fish protein isolate/fish skin gelatin-zinc oxide (ZnO) nanocomposite films, *Food Bioprocess Technol.* 9 (2016) 101–112.
7. M. Arumugam, B. Murugesan, D.k. Chinnalagu, S. Mahalingam, Dual therapeutic approach: biodegradable nanofiber scaffolds of silk fibroin and collagen combined with silver and gold nanoparticles for enhanced bacterial infections treatment and accelerated wound healing, *J. Drug Deliv. Sci. Technol.* 95 (2024) 105620.
8. F. Badii, W. MacNaughtan, J.R. Mitchell, I.A. Farhat, The effect of drying temperature on physical properties of thin gelatin films, *Drying Technol.* 32 (2014) 30–38.
9. C.A. Bashur, L.A. Dahlgren, A.S. Goldstein, Effect of fiber diameter and orientation on fibroblast morphology and proliferation on electrospun poly(d,l-lactic-co-glycolic acid) meshes, *Biomaterials* 27 (2006) 5681–5688.
10. K.D. Bentsen, S.I. Hansen, J. Holm, J. Lyngbye, Abnormalities in folate binding pattern of serum from a patient with megaloblastic anemia and folate deficiency, *Clin. Chim. Acta* 109 (1981) 225–228.
11. A. Bigi, S. Panzavolta, K. Rubini, Relationship between triple-helix content and mechanical properties of gelatin films, *Biomaterials* 25 (2004) 5675–5680.
12. L.F. Bustos, M.A. Judis, F.E. Vasile, O.E. Pérez, Molecular interactions involved in the complexation process between buffalo whey proteins concentrate and folic acid, *Food Chem.* 396 (2022) 133734.
13. J. Chen, L. Li, R. Yi, N. Xu, R. Gao, B. Hong, Extraction and characterization of acid-soluble collagen from scales and skin of tilapia (Oreochromis niloticus), *LWT-Food Sci. Technol.* 66 (2016) 453–459.
14. Z. Chen, X. Mo, C. He, H. Wang, Intermolecular interactions in electrospun collagen–chitosan complex nanofibers, *Carbohydr. Polym.* 72 (2007) 410–418.
15. Z. Chen, X. Mo, C. He, H. Wang, Intermolecular interactions in electrospun collagen–chitosan complex nanofibers, Carbohydr. Polym. 72 (2008) 410–418.
16. D.J. Choi, S.M. Choi, H.Y. Kang, H.-J. Min, R. Lee, M. Ikram, F. Subhan, S.W. Jin, Y.H. Jeong, J.-Y. Kwak, S. Yoon, Bioactive fish collagen/polycaprolactone composite nanofibrous scaffolds fabricated by electrospinning for 3D cell culture, *J. Biotechnol.* 205 (2015) 47–58.
17. B. Ding, H.-Y. Kim, S.-C. Lee, D.-R. Lee, K.-J. Choi, Preparation and characterization of nanoscaled poly(vinyl alcohol) fibers via electrospinning, Fibers Polym. 3 (2002) 73–79.
18. J. Doshi, D.H. Reneker, Electrospinning process and applications of electrospun fibers, J. Electrostat. 35 (1995) 151–160.
19. R. Duan, K. Wang, T. Xu, J. Wei, Y. Liu, J. Zhang, Method for determining 6S-5-methyltetrahydrofolate calcium in collagen membrane materials by high-performance liquid chromatography, CN Patent 116718714A.
20. S.J. Duthie, A. Hawdon, DNA instability (strand breakage, uracil misincorporation, and defective repair) is increased by folic acid depletion in human lymphocytes in vitro, FASEB J. 12 (1998) 1491–1497.
21. A.K. Ekaputra, G.D. Prestwich, S.M. Cool, D.W. Hutmacher, The three-dimensional vascularization of growth factor-releasing hybrid scaffold of poly(ε-caprolactone)/collagen fibers and hyaluronic acid hydrogel, Biomaterials 32 (2011) 8108–8117.

 doi:10.20944/preprints202604.0314.v1




22. M. Erencia, F. Cano, J.A. Tornero, M.M. Fernandes, T. Tzanov, J. Macanás, F. Carrillo, Electrospinning of gelatin fibers using solutions with low acetic acid concentration: effect of solvent composition on both diameter of electrospun fibers and cytotoxicity, J. Appl. Polym. Sci. 132 (2015) n/a–n/a.
23. B.L. Fabián, J.M. Alicia, V.F. Emanuel, P.O. Edgardo, Molecular interactions involved in the complexation process between buffalo whey proteins concentrate and folic acid, Food Chem. 396 (2022) 133734.
24. B. Ghorani, B. Emadzadeh, H. Rezaeinia, S.J. Russell, Improvements in gelatin cold water solubility after electrospinning and associated physicochemical, functional and rheological properties, Food Hydrocolloids 104 (2020) 105740.
25. M. Herrero-Herrero, J.A. Gómez-Tejedor, A. Vallés-Lluch, PLA/PCL electrospun membranes of tailored fibres diameter as drug delivery systems, Eur. Polym. J. 99 (2018) 445–455.
26. T. Huang, Z.-c. Tu, X. Shangguan, H. Wang, X. Sha, N. Bansal, Rheological behavior, emulsifying properties and structural characterization of phosphorylated fish gelatin, Food Chem. 246 (2018) 428–436.
27. S. J, Folate, vitamin B12 and vitamin B6 and one carbon metabolism, J. Nutr. Health Aging 6 (2002) 39–42.
28. V.B. J, G.T. J, M. Rudolf, M.J. I, Comparison of the effect of low-dose supplementation with L-5-methyltetrahydrofolate or folic acid on plasma homocysteine: a randomized placebo-controlled study, Am. J. Clin. Nutr. 77 (2003) 658–662.
29. Z. Jiahui, J. Lian, Y. Jun, C. Xianxiang, S. Mingyue, Y. Qiang, C. Yi, X. Jianhua, Effect of calcium chloride on heat-induced Mesona chinensis polysaccharide-whey protein isolation gels: gel properties and interactions, LWT 155 (2022).
30. A.A. Karim, R. Bhat, Gelatin alternatives for the food industry: recent developments, challenges and prospects, Trends Food Sci. Technol. 19 (2008) 644–656.
31. I. Katouzian, S.M. Jafari, Y. Maghsoudlou, L. Karami, M.H. Eikani, Experimental and molecular docking study of the binding interactions between bovine $\alpha$-lactalbumin and oleuropein, Food Hydrocolloids 105 (2020) 105859.
32. C.S. Ki, D.H. Baek, K.D. Gang, K.H. Lee, I.C. Um, Y.H. Park, Characterization of gelatin nanofiber prepared from gelatin–formic acid solution, Polymer 46 (2005) 5094–5102.
33. P. Klaus, B. Lynn, S. Barry, Folic acid and L-5-methyltetrahydrofolate: comparison of clinical pharmacokinetics and pharmacodynamics, Clin. Pharmacokinet. 49 (2010) 535–548.
34. H.W. Kwak, M. Shin, J.Y. Lee, H. Yun, D.W. Song, Y. Yang, B.-S. Shin, Y.H. Park, K.H. Lee, Fabrication of an ultrafine fish gelatin nanofibrous web from an aqueous solution by electrospinning, Int. J. Biol. Macromol. 102 (2017) 1092–1103.
35. S.J. Lee, J. Liu, S.H. Oh, S. Soker, A. Atala, J.J. Yoo, Development of a composite vascular scaffolding system that withstands physiological vascular conditions, Biomaterials 29 (2008) 2891–2898.
36. L. Lei-Gen, H. Ji-Huan, Solvent evaporation in a binary solvent system for controllable fabrication of porous fibers by electrospinning, Therm. Sci. 21 (2017) 1821–1825.
37. V. Leung, H. Yang, F. Ko, Nanofibers for ligament and tendon tissue regeneration, in: Biomedical Textiles for Orthopaedic and Surgical Applications, Elsevier, 2015, pp. 91–118.
38. W. Li, M. Yu, S. Luo, H. Liu, Y. Gao, J.X. Wilson, G. Huang, DNA methyltransferase mediates dose-dependent stimulation of neural stem cell proliferation by folate, J. Nutr. Biochem. 24 (2013) 1295–1301.
39. F. Lingling, F. Jin, L. chunyang, Extraction and structural characteristics of type I collagen from Rhopilema esculenta, Sci. Technol. Food Ind. 42 (2021) 15–21.
40. H. Liu, G.-w. Huang, X.-m. Zhang, D.-l. Ren, J.X. Wilson, Folic acid supplementation stimulates Notch signaling and cell proliferation in embryonic neural stem cells, J. Clin. Biochem. Nutr. 47 (2010) 174–180.
41. B. Mansooreh, J.B. Moein, Z. Ali, Folic acid may be a potential addition to diabetic foot ulcer treatment - a hypothesis, Int. Wound J. 8 (2011) 658–660.
42. Y. Mou, X. Lei, F. Xing, J.-p. Gao, G. Peng, G. Zhang, M. Wang, Preparation and biological evaluation of electrospun collagen membrane, Chin. J. Process Eng. 18 (2018) 1075–1081.
43. P.F. Nur, U. Sana, Y. Kenan, H. Motahira, K. IckSoo, Fabrication and characterization of electrospun folic acid/hybrid fibers: in vitro controlled release study and cytocompatibility assays, Polymers 13 (2021) 3594.

 doi:10.20944/preprints202604.0314.v1




44. J. Padrão, R. Silva, L.R. Rodrigues, F. Dourado, S. Lanceros-Méndez, V. Sencadas, Modifying fish gelatin electrospun membranes for biomedical applications: cross-linking and swelling behavior, Soft Mater. 12 (2014) 247–252.
45. J. Padrão, R. Machado, M. Casal, S. Lanceros-Méndez, L.R. Rodrigues, F. Dourado, V. Sencadas, Antibacterial performance of bovine lactoferrin-fish gelatine electrospun membranes, Int. J. Biol. Macromol. 81 (2015) 608–614.
46. C. Pathum, O. Gun-Woo, H. Seong-Yeong, K. Se-Chang, K. Tae-Hee, K. Min-Sung, J. Won-Kyo, Electrospun porous bilayer nano-fibrous fish collagen/PCL bio-composite scaffolds with covalently cross-linked chitooligosaccharides for full-thickness wound-healing applications, Mater. Sci. Eng. C 121 (2021) 111871.
47. Z.-y. Qin, X.-W. Jia, Q. Liu, B.-h. Kong, H. Wang, Fast dissolving oral films for drug delivery prepared from chitosan/pullulan electrospinning nanofibers, Int. J. Biol. Macromol. 137 (2019) 224–231.
48. F. Sara, S. Silvia, S.A. Calogero, C. Andrea, R. Lia, C. Iriczalli, G. Vincenzo, V. Alessio, V. Claudia, Topographical and biomechanical guidance of electrospun fibers for biomedical applications, Polymers 12 (2020).
49. P. Songchotikunpan, J. Tattiyakul, P. Supaphol, Extraction and electrospinning of gelatin from fish skin, Int. J. Biol. Macromol. 42 (2007) 247–255.
50. J. Stitzel, J. Liu, S.J. Lee, M. Komura, J. Berry, S. Soker, G. Lim, M. Van Dyke, R. Czerw, J.J. Yoo, A. Atala, Controlled fabrication of a biological vascular substitute, Biomaterials 27 (2006) 1088–1094.
51. M. Sun, P. Ma, C. Chen, Z. Pang, Y. Huang, X. Liu, P. Wang, Physiochemical characteristics, morphology, and lubricating properties of size-specific whey protein particles by acid or ion aggregation, Int. J. Biol. Macromol. 252 (2023) 126346.
52. S. Torres-Giner, E. Gimenez, J.M. Lagaron, Characterization of the morphology and thermal properties of Zein Prolamine nanostructures obtained by electro spinning, Food Hydrocolloids 22 (2008) 601–614.
53. M. Vahid, F. Milad, S. Mohammad, S. Nafiseh, E.-D. Zahra, Fast-dissolving antioxidant nanofibers based on Spirulina protein concentrate and gelatin developed using needleless electrospinning, Food Biosci. 47 (2022).
54. G. Vincenzo, C. Valentina, A. Luigi, Bicomponent electrospun scaffolds to design extracellular matrix tissue analogs, Expert Rev. Med. Devices 13 (2016) 83–102.
55. Q. Wang, Y. Wei, W. Li, X. Luo, X. Zhang, J. Di, G. Wang, J. Yu, Polarity-dominated stable N97 respirators for airborne virus capture based on nanofibrous membranes, Angew. Chem. Int. Ed. 60 (2021) 23756–23762.
56. B. Weiwei, Z. Youzhu, Y. Guibo, W. Jialin, The structure and property of the electrospinning silk fibroin/gelatin blend nanofibers, e-Polymers 8 (2008).
57. P. Wen, D.-H. Zhu, H. Wu, M.-H. Zong, Y.-R. Jing, S.-Y. Han, Encapsulation of cinnamon essential oil in electrospun nanofibrous film for active food packaging, Food Control 59 (2016) 366–376.
58. S. Wongsasulak, S. Pathumban, T. Yoovidhya, Effect of entrapped $\alpha$-tocopherol on mucoadhesivity and evaluation of the release, degradation, and swelling characteristics of zein–chitosan composite electrospun fibers, J. Food Eng. 120 (2014) 110–117.
59. L. Xiaoran, X. Jingwei, Y. Xiaoyan, X. Younan, Coating electrospun poly(epsilon-caprolactone) fibers with gelatin and calcium phosphate and their use as biomimetic scaffolds for bone tissue engineering, Langmuir 24 (2008) 14145–14150.
60. Y.Z. Zhang, J. Venugopal, Z.-M. Huang, C.T. Lim, S. Ramakrishna, Crosslinking of the electrospun gelatin nanofibers, Polymer 47 (2006) 2911–2917.
61. J. Zhou, Effects of folic acid on diabetes-induced delayed wound healing in mice, Master Thesis, 2014.